Nuclear Engineering and Technology 53 (2021) 1642–1651

Contents lists available at ScienceDirect

Nuclear Engineering and Technology

journal homepage: www.elsevier.com/locate/net

Original Article

Effect of different tungsten compound reinforcements on the electromagnetic radiation shielding properties of neopentyl glycol polyester

Ömer Can, Ezgi Eren Belgin*, Gul Asiye Aycik

Chemistry Department, Mugla Sitki Koçman University, Kotekli Campus, 48000, Mugla, Turkey

ARTICLE INFO

Article history:
Received 17 July 2020
Received in revised form
23 October 2020
Accepted 4 November 2020
Available online 11 November 2020

Keywords:
Electromagnetic radiation
Radiation shielding
Composite shielding
Tungsten
Neopentyl glycol polyester

ABSTRACT

In this study, isophtalic neopentyl glycol polyester (NPG-PES) based composites with different loading ratios of pure tungsten metal (W), tungsten (VI) oxide (WO_3), tungsten boron (WB) and tungsten carbide (WC) composites were prepared as alternative shielding materials for ionizing electromagnetic radiation (IEMR) shielding. Structural characterizations of the composites were done. Gamma spectrometric analysis of composites for 80–2000 keV energy range was performed and their usability as IEMR shielding was discussed. As a result, the produced composites showed a shielding performance of 60–100% of the lead (the most widely used IEMR shielding material) depending on the reinforcement material, reinforcement loading rate and experimental conditions. Thus, it was reported that produced composites could be an alternative to lead shieldings that have several disadvantages as toxic properties, difficulty of processing and inelasticity.

1. Introduction

The most important factor that reduces the exposured radiation dose is to put a proper shield between the radiation source and the target. The material to be used in shielding design differs according to the type and energy of the radiation to be shielded. Ionizing electromagnetic radiation (IEMR), such as gamma and X-rays, has high penetrating ability and energy high enough to cause ionization in the matter. The common feature of IEMR shielding materials is that they have high density, high atomic number and closed packed crystal structure [1]. Today, the most common shielding materials used for IEMR are lead and lead additive materials. This is because lead has high IEMR attenuation performance and low cost. However, lead has disadvantages such as high weight, toxic feature, difficulty of processing and inelasticity. For this reason, in recent years, it has become important to develop alternative shielding materials that are lighter, flexible, malleable, having high chemical resistance and mechanical strength, which are not harmful to human health and that will remove the disadvantages of lead [2–4].

One of these alternative materials is tungsten which is a transition metal with atomic number of 74 and atomic weight of 183.85 $gmol^{-1}$. It is also one of the heaviest elements with a density of 19.3 gcm^{-3} at 20 °C. It has high corrosion resistance, high heat/electrical conductivity and low expansion coefficient [5]. For these reasons, tungsten is an element that can be used as an alternative to lead for IEMR shielding. However, tungsten is expensive and metallic processing difficulties limits the use of it as pure form that is why more tungsten alloys are studied in IEMR shielding.

In studies on the use of tungsten alloys as shielding material [6], it was reported that tungsten heavy alloys (W–Ni–Fe, W–Ni–Cu–Fe) are 30–40% more effective in IEMR shielding than lead. In other study, low temperature sintered tungsten, tungsten carbide, tungsten-copper alloy and lead's shielding properties were compared and it was found that tungsten-copper alloy gave better shielding properties than lead [7]. Lee stated that lithium hydride-tungsten composite can be used as a very light material for the shielding of gamma rays [8].

How much a shielding material will attenuate IEMR depends on the properties of the material used, as well as the energy of the IEMR. Predominant interaction mechanisms of IEMR with shielding material differ due to energy. At low energies photoelectric effect is predominant mechanism while Compton scattering is predominant for intermediate energies and pair production is predominant for high energies [9].

In this study, isophtalic neopentyl glycol polyester (NPG-PES)

* Corresponding author.
E-mail address: ebelgin@mu.edu.tr (E. Eren Belgin).

https://doi.org/10.1016/j.net.2020.11.006

based composites with different reinforcement loading ratios of pure tungsten metal (W), tungsten (VI) oxide (WO_3), tungsten boron (WB) and tungsten carbide (WC) composites were prepared. NPG-PES was choosen as matrix material of the composites because of its high chemical and mechanical resistance property [10]. After preparation of the composites structural characterizations of the composites were done by scanning electron microscope examinations and Fourier transform infrared spectroscopy analysis. Since the IEMR shielding performances will be different at different IEMR energies for the reason described above, gamma spectrometric analysis of composites for 80–2000 keV energy range was performed and their usability as IEMR shielding was discussed. In the literature, it has been observed that NPG-PES's radiation shielding properties were not studied before. In addition, tungsten reinforced composite structures are not studied for different IEMR energies instead they are studied mostly for individual energies or neutron attenuation properties.

2. Experimental

2.1. Composite constituents

In the study, commercially available isophthalic neopentyl glycol (NPG) based unsaturated polyester (NPG-PES) resin was used as composite matrix material. The most obvious advantage of NPG-PES from polyesters is being chemical resistant even at high temperatures. Another superior feature is that it provides products with high physical strength. It is therefore suitable for use in areas where low weight but high mechanical strength is important. Its hydrolytic stability is very high. It has high heat resistance, superior electrical properties and high disruptive voltage. In addition, dielectric loss is low and does not cause a significant loss from its mechanical values at high temperatures [10].

In the study, pure (99%) tungsten metal and 3 tungsten compounds (WO_3, WB and WC) were used as reinforcement materials. Thus, it was aimed to compare the shielding properties of the different compounds as well as to eliminate the difficulties of treating and processing tungsten. The properties of the reinforcement materials used are given in Table 1.

2.2. Composite production

Composites are produced by the radicalic polymerization method. As a radical source, 1.25% methyl ethyl ketone peroxide (MEKP) was used, and 0.75% metal catalyst (cobalt octoate-Coct) was used as cross-linking reaction catalyst. Reinforcements were loaded at 20, 30, 40, 50 and 60% for each reinforcement material.

The reinforcement materials and NPG-PES were weighed sensitively with a calibrated electronic scale and then mixed with a mechanical mixer at a speed of 120 rpm. While mixing was in progress, MEKP and Coct were added to the polymerization medium and cross-linking reactions were started to form a 3D network structure in the resin. In order to prevent precipitation of the reinforcement materials that are dense with respect to the polymer during the molding process, the mixing process was continued until the gelling point where the viscous liquid of NPG-PES became gel consistency due to cross linking process. Later, the composite mixtures were taken into the molds and cured at room temperature for 24 h and at 80 °C for 8 h in a constant temperature cabin for completion of cross linking [11–13].

The codes used for the composites produced in the study and the composite constituents are given in Table 2.

2.3. Composite characterization

2.3.1. Composite homogeneity tests

One of the most important problems in composite preparation by using low-density polymer and high-density reinforcement materials via radical polymerization technique is that heavy reinforcement particles settle to the bottom of the mixture with the effect of gravity until cross-linking is completed. Thus, the reinforcement materials cannot be distributed homogeneously in the polymer, phase separations are observed and heterogeneous composite structures are formed.

Since the first condition that must be met in order to obtain correct results in characterization studies in the composite materials is a homogeneous composite structure, four parallel composite materials were produced at the same reinforcement loading rates to control the homogeneity of the composite materials produced. Energy dependent IEMR attenuation performances of composite materials produced were measured by gamma spectrometric method. The results were compared with regression analysis by calculating the determination coefficient (R^2) that is the proportion of the variance in the dependent variable that is predictable from the independent variable(s).

2.4. Structural characterization

The internal structure analysis of composites was performed using scanning electron microscope (SEM/JEOL-JSM-7600F). The microstructures obtained, as a result of the analysis performed for both polished and fractured surfaces, were evaluated. The sizes and grain shapes of the phases and if the phases were homogeneously distributed in the composite material were determined.

Fourier transform infrared spectroscopy (FTIR/Thermo Scientific-Nicolet-1510) analyses were performed to understand the relationship between composite reinforcement materials and matrix. As a result of the analyses, functional group changes that may occur in the composite structure were examined.

2.5. Gamma spectrometric characterization

In the study, gamma spectrometric method was used to determine the IEMR shielding properties of composites. Due to its high resolving power and wide counting angle, a well-type high purity germanium (HPGe) semiconductor detector with a volume of 110 cm^3 and a resolution of 3.78 keV (Co-60-1.33 MeV) was preferred as the spectrometer detector.

The gamma spectrum from the multichannel analyser connected to the detector was analysed using computer software

Table 1
Properties of used reinforcement materials.

Reinforcement material	Density (gcm^{-3})	Molecular Weight ($gmol^{-1}$)	Crystal structure	Origin
W	19.3	183.8	Body centered cubic	Merck
WO_3	7.16	231.8	Tetragonal	Merck
WB	15.3	194.7	Orthorombic	Merck
WC	15.6	195.85	Hexagonal	Merck

Table 2
Composite codes and constituents.

Composite code	Reinforcement type	Reinforcement: Matrix ratio
RW20; RW30; RW40; RW50; RW60	Metallic W	20:80; 30:70; 40:60; 50:50; 60:40
RWO20; RWO30; RWO40; RWO50; RWO60	WO_3	20:80; 30:70; 40:60; 50:50; 60:40
RWB20; RWB30; RWB40; RWB50; RWB60	WB	20:80; 30:70; 40:60; 50:50; 60:40
RWC20; RWC30; RWC40; RWC50; RWC60	WC	20:80; 30:70; 40:60; 50:50; 60:40

'ORTEC-Omnigam B-30'. In order to prevent detector efficiency errors, which is the biggest problem encountered in gamma spectrometric measurements, all measurements were done relatively by comparing initial and residual intensities of the radionuclide source. A cylindrical lead shield, placed onto the detector to allow the detector to count only the gamma rays coming through the composites by blocking the gamma rays coming through to the detector from other directions. Then the radionuclide source was placed on this lead shield and composites were placed into the lead shield between the source and the detector. Details of the measurement method were given previously [11–13].

To test the usability of composites for different IEMR energy ranges as shielding material, gamma spectrometric measurements were held for three different IEMR energy zones as low (0–500 keV), intermediate (500–1100 keV) and high (>1100 keV). Since the energy of gamma rays is intermittent and characteristic for each nucleus, it was possible to held analysis individually and simultaneously for different IEMR energies with the use of mixed nuclide point source. The used source was containing Am-241, Cd-109, Co-57, Ce-139, Sn-113, Cs-137, Y-88 and Co-60 radionuclides with photopeaks of different energies (88, 122, 166, 392, 662, 898, 1173, 1333, 1836 keV).

Intensities (the number of counts per second) recorded by the detector for the radioactive source (intensity before interaction), the source + composites or lead (intensity after interaction) were calculated by using manually selected net areas under the detected photopeaks of the radionuclides of the mixed source via software of the detector. The attenuation rate (F%, ratio of the intensity lost of incoming radiation to its initial intensity, %) and mass attenuation coefficient (μ_M, attenuation coefficient per unit mass of material, cm^2g^{-1}) values of the composites and elemental lead were then calculated via Eqs. (1) and (2) after determination of intensity of radiation before interaction (I_0) and after interaction (I) with the shielding material.

$$\%F = \frac{(I_0 - I)}{I_0} \times 100 \quad (1)$$

$$\mu M = \ln\left(\frac{I0}{I}\right) \Big/ x\rho \quad (2)$$

In Equation (2), x represents thickness and ρ represents density of the material. Evaluation methods of the F% and μ_M values described detailed in the previous studies [11–13].

3. Results and discussion

3.1. Homogeneity test results

In the study, two parallel sample groups were prepared and each parallel sample groups were produced as five sets of samples for homogeneity tests. Attenuation rates (%) of the parallel samples were calculated by gamma spectrometric method, mean value of five set is accepted as group value and results are given with respect to photopeak energy for 60% reinforced composites (Table 3).

The calculated attenuation rates (%) of the sample groups were plot with respect to each other for regression analysis and determination coefficients (R^2) of the lines were calculated.

In Fig. 1, the graphs obtained for different composites at 60% reinforcement loading ratios, where the homogeneity condition is the most difficult to meet due to the high reinforcement loading rate, are given.

R^2 values of the composites with the highest reinforcement loading rate, that is the most difficult to achieve homogeneity, vary between 0.9984 and 0.9999 (Fig. 1) and the average R^2 value was found to be 0.9991. The insignificantly deviation from the value of 1 may arise from the weighing errors and the parameters in the production process. The proximity of R^2 values to 1, which should be provided for perfect homogeneity, showed that composites prepared in the study met the homogeneity condition.

3.2. Structural characterization

Within the scope of structural characterization, FTIR analysis of composite matrix (NPG-PES) and composites have been performed. FTIR spectra of composites with 60% reinforcement loading ratio, expected to be the most likely absorbance value change, are given in Fig. 2. Characteristic transmission bands of NPG-PES were seen in the FTIR spectrum (approximately at 1721, 1230, 698 cm^{-1}). The same characteristic transmission bands were also seen in composites produced without showing any significant shift value. In the absorbance values of these bands, there were acceptable changes due to possible changes in the bond densities in the interested part of the sample. These results showed that there was no chemical interaction between reinforcement materials and composite matrix NPG-PES. Reinforcement particles, as expected, were physically attached between the NPG-PES during crosslinking reactions.

SEM analysis of the composite materials was made for both fractured and polished surfaces of the composite materials. Thus, the surface morphology of composites, the distribution of reinforcement particles in the matrix, phase separations, grain boundaries were investigated. The SEM photos obtained are given for 60% reinforced composites with the highest reinforcement loading ratio (Fig. 3).

As can be seen from the fractured surface SEM photographs of composites, not much gap was observed in the composites due to polymer matrix hardening during production process and grain removal on fractured surfaces. In polished surface photographs, reinforcement particles and matrix material could be easily distinguished, no phase separation was observed in the reinforcement particle-matrix interface that shows a good reinforcement-matrix adhesion. It was also seen that the reinforcing grains are distributed homogeneously in the matrix.

3.3. Gamma spectrometric characterization

Attenuation of the IEMR by a shielding material occurs via interaction of IEMR with shielding material's atoms and atomic electrons as it travels through the material. IEMR loses some of its energy and its energy drops to acceptable levels when it leaves the shielding material with every interaction. However, the amount of interaction will depend on both the properties of the shielding

Table 3
Parallel sample group attenuation rate (%) results of the composites prepared with 60% reinforcement loading ratios.

Composite Code	Attenuation Rates (%)							
	88 keV	122 keV	166 keV	392 keV	662 keV	1173 keV	1333 keV	183 keV
RW60-Group 1	99.99	86.84	69.95	48.28	20.92	15.47	13.40	43.86
RW60-Group 2	99.99	85.75	69.38	44.60	20.51	15.98	12.97	41.83
RWO60-Group 1	99.99	83.50	73.29	61.76	21.80	19.40	15.74	39.67
RWO60-Group 2	99.99	83.02	73.86	61.14	22.03	19.85	15.49	40.47
RWB60-Group 1	99.99	87.36	67.07	67.69	21.86	14.16	19.27	44.42
RWB60-Group 2	99.99	87.48	67.30	66.83	21.92	14.61	19.08	44.54
RWC60-Group 1	99.99	94.76	80.52	66.49	18.79	11.26	18.25	40.35
RWC60-Group 2	99.99	93.51	76.74	67.76	18.90	11.14	17.32	39.05

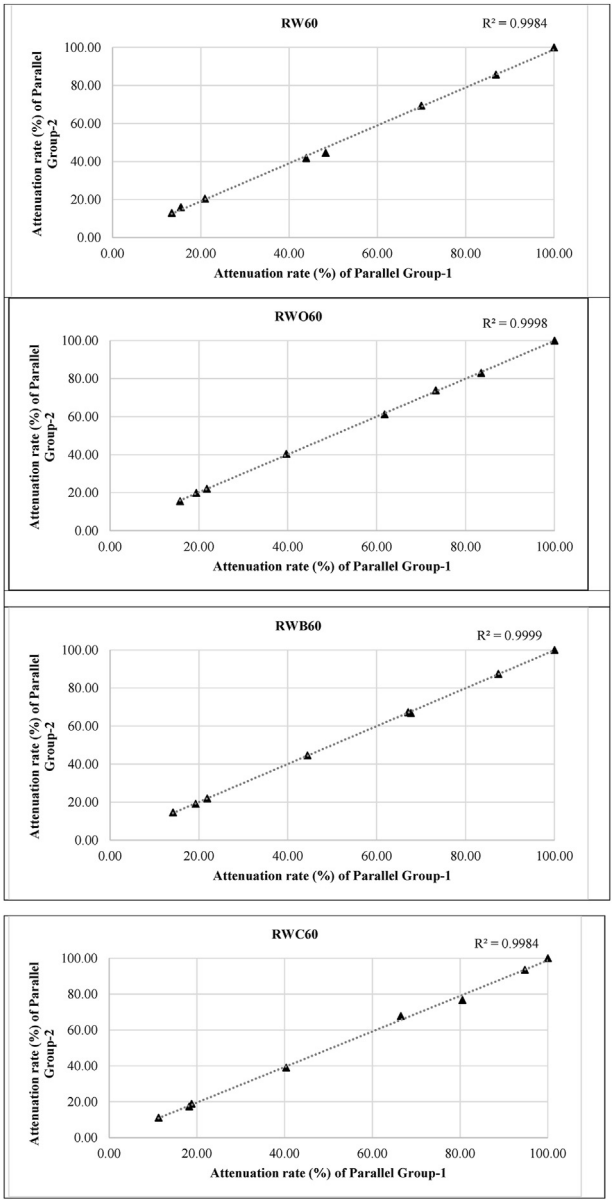

Fig. 1. Regression analysis graphs and R^2 values for attenuation rates (%) of composites prepared with 60% reinforcement loading ratios.

material and the energy of the IEMR.

The high atomic number (Z) of the IEMR shielding material is one of the top priority features. Materials containing elements with suitable atomic numbers are used for shielding according to the energy of the emitted radiation. Interaction mechanisms of IEMR with matter at different energies are also different. At low energies, the photoelectric effect is the predominant interaction type and its photoelectric absorption cross section is proportional to the Z^5 per electron of the shielding material in the range of 0.001–0.5 MeV. In medium energies, in the range of 0.5–2.0 MeV where Compton scattering is the predominant interaction type, the cross section of the shielding material per electron is proportional to Z. For high photon energies (>1.02 MeV), the pair formation is the predominant interaction, and the variation of the cross section with the photon energy is complex, but Z^2 is proportional [9].

Apart from the high atomic number, the density and crystal structure of the shielding material are also the primary features for proper shielding. Essentially, the density of the material is determined by atomic numbers of the elements that make up the material and the crystal structure of the material. If the amount of spaces between atoms in the crystal structure is high, these spaces will cause most of the incoming radiation to proceed without being absorbed in the material. Thus, the materials with closed packed crystal structure with fewer spaces have better shielding properties.

The attenuation rates (%) and mass attenuation coefficients (cm^2g^{-1}) of pure lead, which is the commercially widely used IEMR shielding material, and produced composites, were calculated for different energies (88, 122, 166, 392, 662, 1173, 1333, 1830 keV) and the results were interpreted in the light of the information mentioned above.

As part of the evaluation of the shielding performance of the composites produced in the study, first, the attenuation rates (%), which indicate how much of the energy of the incoming IEMR could be absorbed, were calculated and the results are given (Figs. 4–7).

The İEMR attenuation rates of almost all materials in the range of 88–166 keV were higher than the attenuation rates in higher energies (Figs. 4–7). This is because there is a high probability of photoelectric interaction in the range of 0–400 keV and the energy loss in photoelectric interaction is proportional to Z^5. Therefore, as the Z value increases, the shielding performance of the materials had increased as energy loss of IEMR would increase by photoelectric interaction.

Since the IEMR attenuation feature in the Compton region (400–1022 keV) is proportional to Z, the increase in the Z value of the composites did not affect the IEMR attenuation rates significantly for intermediate energies.

In energies greater than 1022 keV, the phenomenon of pair production is predominant. Since the rate of IEMR attenuation is proportional to Z^2 for pair production interaction, it was seen that the IEMR attenuation rates has started to increase slowly again at >1022 keV energies.

IEMR attenuation rates were increased as the reinforcement loading ratio increased for the low, medium and high IEMR energy

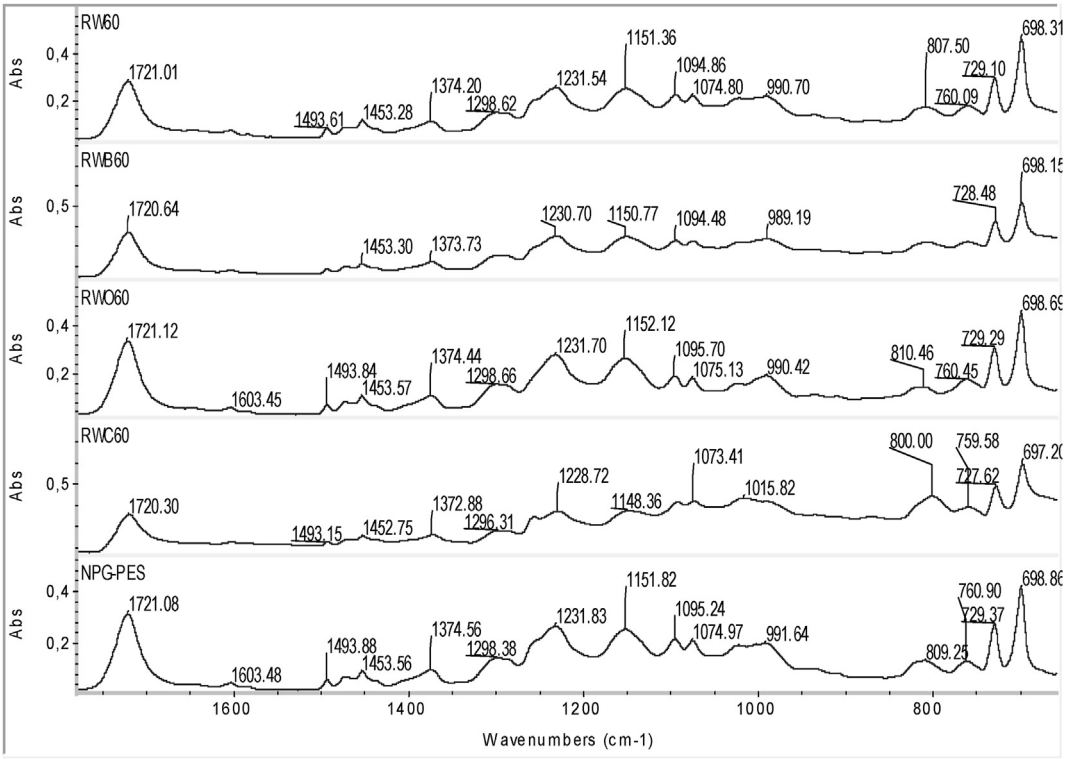

Fig. 2. FTIR spectra of 60% reinforced composites and NPG-PES.

regions and for each type of reinforcement used in the study (Figs. 4–7). This result also showed that the critical loading rate has not been exceeded although high reinforcement loading ratios such as 60% have been achieved. If the critical loading rate had been exceeded, since the enough amount of polymer matrix could not be found in the polymerization environment to cover each reinforcement particle, it would be expected to form gaps in the structure that leads a decrease the IEMR shielding performance. However, such a decrease was not observed for the composites produced.

60% reinforced composites' (having the highest attenuation rates), composite matrix NPG-PES's and lead's (widely used shielding material) attenuation rates were compared (Fig. 8). It was aimed to show different tungsten compound reinforcement's effect on NPG-PES matrix' IEMR shielding properties.

Lead showed higher IEMR attenuation performance in all IEMR energies due to its high density and closed packed crystal structure (Fig. 8). At 88 keV, all composites reached the shielding performance of the lead. Pure tungsten reinforced composites, which are expected to show the highest performance due to their density, could not perform highest performance as expected due to tungsten's body centered cubic (bcc) crystal structure and generally showed lower shielding performance than other composites. WC reinforced composites generally showed high shielding performance since they have both high density and closed packed hexagonal crystal structure properties. Approximately 84% of the lead performance was reached for the same thickness by the RWB60 composite in 1836 keV, which is the highest energy studied and therefore the most difficult to attenuate. In addition, with the use of reinforcement, the shielding performance of NPG-PES has been increased by 11 times in this energy.

As mentioned earlier, the primary requirement is the high density of the shielding material for high IEMR attenuation performance, the densities of composites produced in the study were determined by Archimedes method [14] and are given in Table 4.

As seen in Table 4, the composites with highest density for the same reinforcement loading ratio were pure tungsten reinforced composites. WC, WB and WO_3 loaded composites follow them respectively according to reinforcement densities.

Lead showed higher attenuation performance for unit thickness than the composites produced in the study but lead shields have difficulty in use due to its low mechanic stability and high toxicity. In addition, the high weight of lead aprons and lead blocks becomes a disadvantage especially in application areas where wearable or mobile shielding is required. Lead aprons are uncomfortable, transportation of lead blocks are difficult, lead doors deforms over time and even lead rooms shielded with lead blocks can distrupt the building statics due to their high weight. For this reason, when comparing IEMR shielding materials, it is important to compare their shielding performance not only for unit thickness but also unit mass. The mass attenuation coefficient (cm^2g^{-1}), which express the attenuation performance per unit mass is a suitable parameter for this comparasion. In other words, if a material has high μ_M value, the shield made from the material would have low weight. Therefore, μ_M values of 60% reinforced composites are compared with lead values (Fig. 9) in the study. The comparison was made on average values of results by accepting them as low (88–166 keV), medium (392–662 keV) and high (1173–1836 keV) energy zones in order to be more plain and understandable.

The composite group having the lowest densities produced were WO_3 reinforced composites with density of 4.74 gcm^{-3} for highest loading ratio. For this reason, RWO60 composite had the highest μ_M value per unit mass due to its lightness as well as its relatively high shielding performance (Fig. 9). In fact, WO_3 loaded composites had lower attenuation rates (%) than other composites produced but at the same time their densities were lower than them. Thus, when the μ_M values that is the performance per unit mass of the materials are considered, WO_3 reinforced composites seemed as the composites having the highest μ_M values. Pure

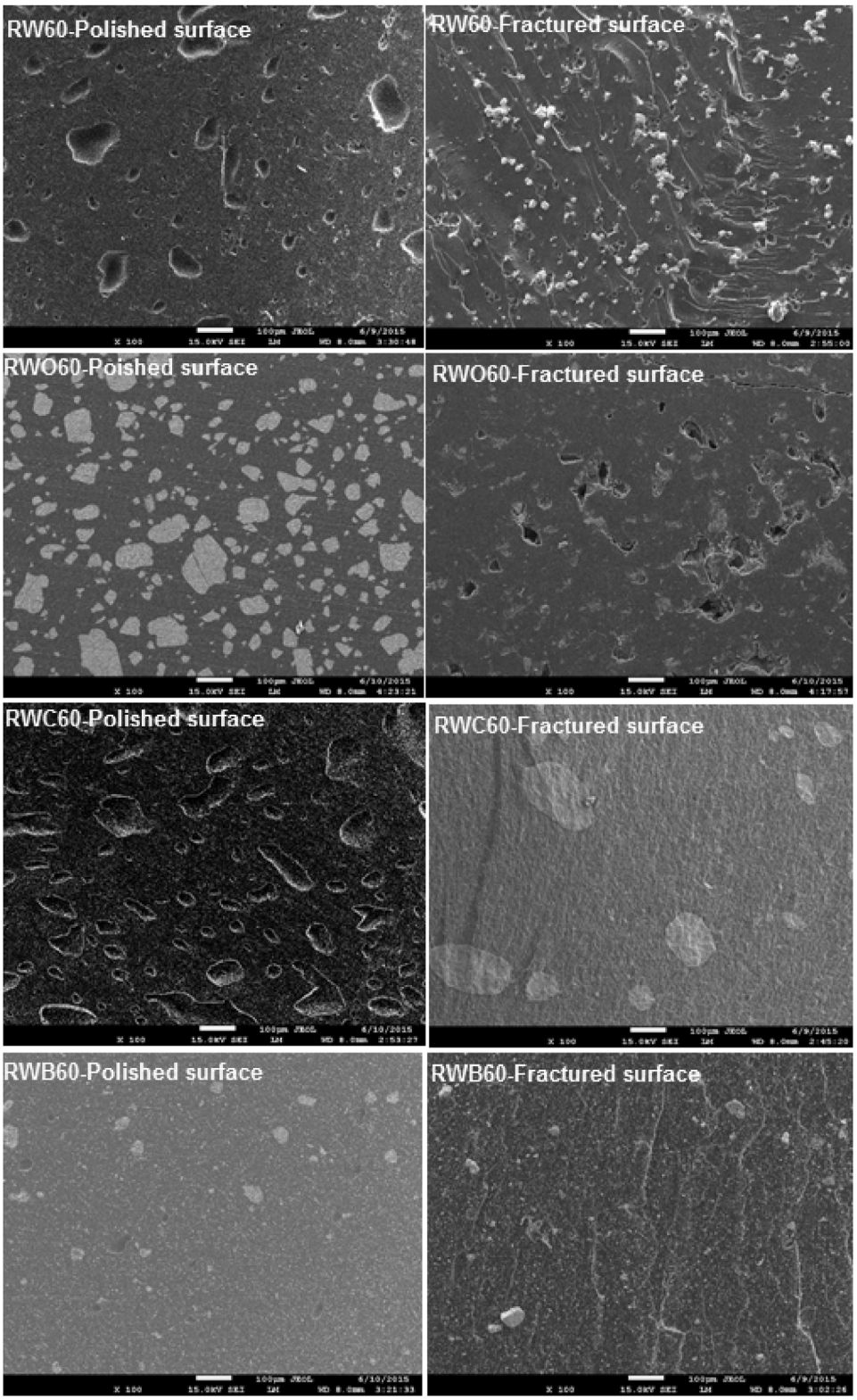

Fig. 3. Fractured and polished surface SEM photographs of composites with 60% reinforcement loading ratio at 100X magnification.

tungsten reinforced composites had the lowest μ_M values due to the high density of tungsten and its body centered cubic crystal structure leading low shielding performance.

4. Conclusion

In this study, NPG-PES matrix was reinforced with different tungsten compounds (W, WO_3, WC and WB), and composite IEMR shielding materials were produced. Composites were produced by

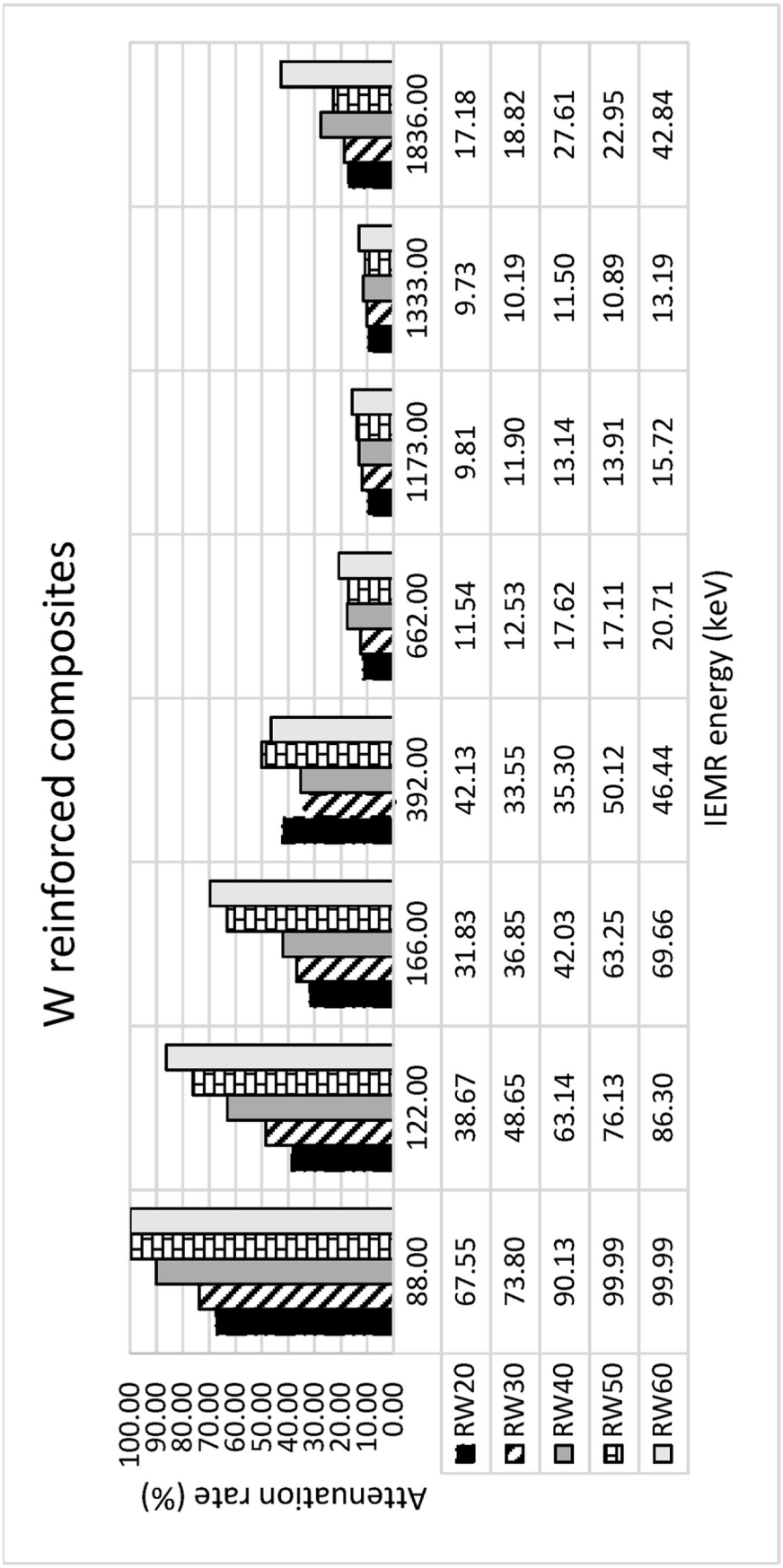

Fig. 4. Attenuation rates of W reinforced composites.

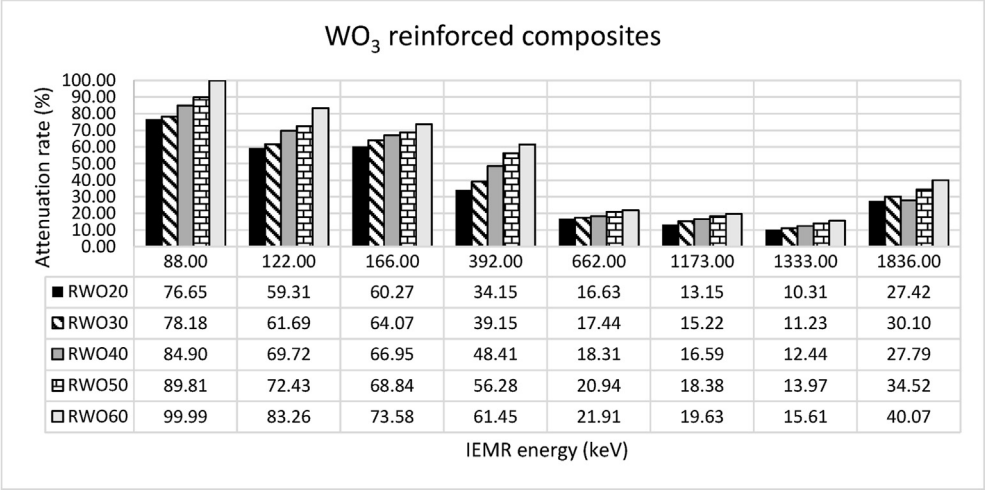

	88.00	122.00	166.00	392.00	662.00	1173.00	1333.00	1836.00
RWO20	76.65	59.31	60.27	34.15	16.63	13.15	10.31	27.42
RWO30	78.18	61.69	64.07	39.15	17.44	15.22	11.23	30.10
RWO40	84.90	69.72	66.95	48.41	18.31	16.59	12.44	27.79
RWO50	89.81	72.43	68.84	56.28	20.94	18.38	13.97	34.52
RWO60	99.99	83.26	73.58	61.45	21.91	19.63	15.61	40.07

Fig. 5. Attenuation rates of WO_3 reinforced composites.

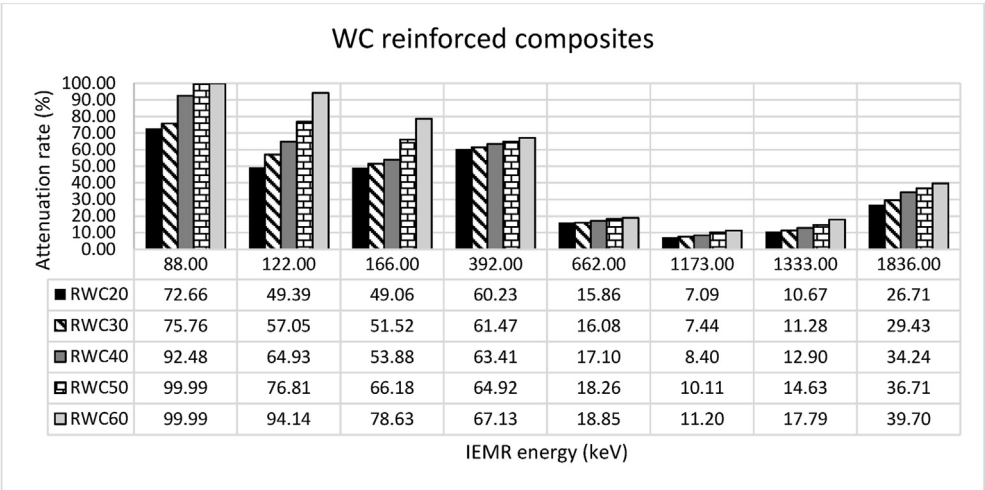

	88.00	122.00	166.00	392.00	662.00	1173.00	1333.00	1836.00
RWC20	72.66	49.39	49.06	60.23	15.86	7.09	10.67	26.71
RWC30	75.76	57.05	51.52	61.47	16.08	7.44	11.28	29.43
RWC40	92.48	64.93	53.88	63.41	17.10	8.40	12.90	34.24
RWC50	99.99	76.81	66.18	64.92	18.26	10.11	14.63	36.71
RWC60	99.99	94.14	78.63	67.13	18.85	11.20	17.79	39.70

Fig. 6. Attenuation rates of WC reinforced composites.

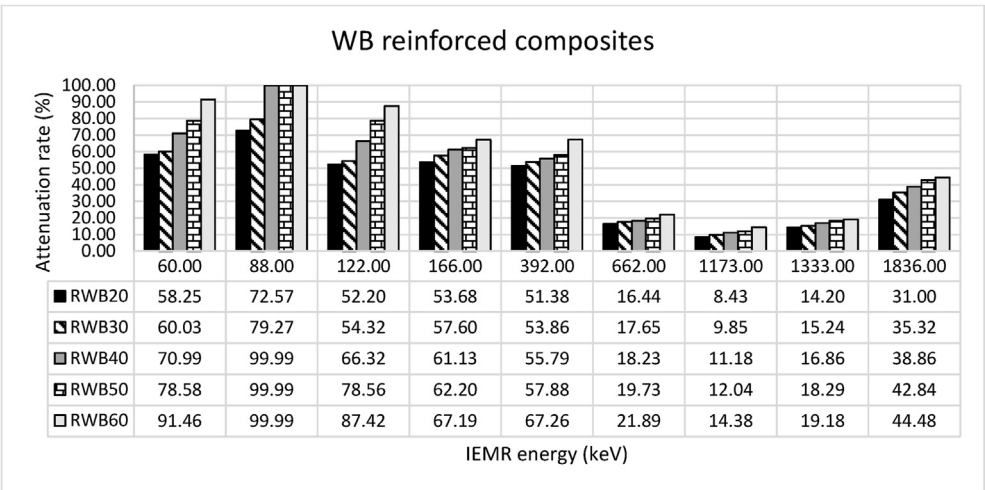

	60.00	88.00	122.00	166.00	392.00	662.00	1173.00	1333.00	1836.00
RWB20	58.25	72.57	52.20	53.68	51.38	16.44	8.43	14.20	31.00
RWB30	60.03	79.27	54.32	57.60	53.86	17.65	9.85	15.24	35.32
RWB40	70.99	99.99	66.32	61.13	55.79	18.23	11.18	16.86	38.86
RWB50	78.58	99.99	78.56	62.20	57.88	19.73	12.04	18.29	42.84
RWB60	91.46	99.99	87.42	67.19	67.26	21.89	14.38	19.18	44.48

Fig. 7. Attenuation rates of WB reinforced composites.

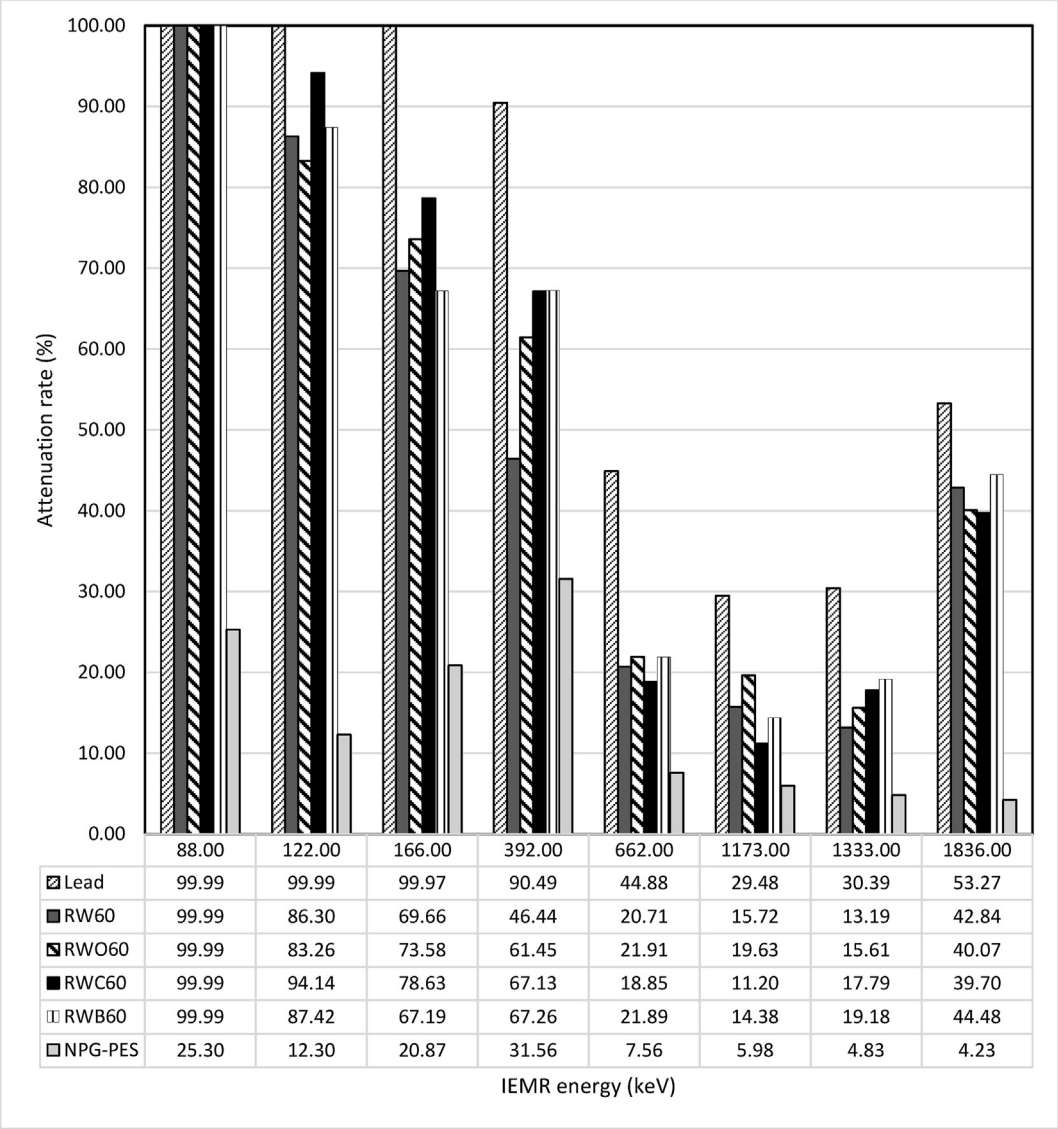

	88.00	122.00	166.00	392.00	662.00	1173.00	1333.00	1836.00
Lead	99.99	99.99	99.97	90.49	44.88	29.48	30.39	53.27
RW60	99.99	86.30	69.66	46.44	20.71	15.72	13.19	42.84
RWO60	99.99	83.26	73.58	61.45	21.91	19.63	15.61	40.07
RWC60	99.99	94.14	78.63	67.13	18.85	11.20	17.79	39.70
RWB60	99.99	87.42	67.19	67.26	21.89	14.38	19.18	44.48
NPG-PES	25.30	12.30	20.87	31.56	7.56	5.98	4.83	4.23

Fig. 8. Attenuation rates of 60% reinforced composites, composite matrix NPG-PES and commercially used IEMR shielding material lead.

Table 4
Experimental densities of the produced composites.

Reinforcement loading ratio (%)	Reinforcement type and density (gcm^{-3})			
	W	WO_3	WB	WC
20	4.71	2.29	2.65	3.91
30	6.53	2.9	3.44	5.43
40	8.36	3.52	4.24	6.89
50	10.18	4.13	5.03	8.34
60	12	4.74	5.82	9.8

the radicalic polymerization method using different reinforcement loading ratios ranging from 20% to 60%. It was understood by homogeneity tests and SEM analysis that homogeneous structures were constituted. FTIR analysis also showed that the relationship between matrix and reinforcement particles was physical.

IEMR shielding performances of composites were determined by gamma spectrometric measurements and compared with both conventional shielding material lead and composite matrix NPG-PES. The results are summarized in Table 5.

RWC60 composite, which was approximately 1.16 times lighter than lead, showed the highest performance for the low IEMR energy region when the same thickness of shielding material was used. For the medium and high IEMR energy zones, the RWB60 composite showed the highest performance that was approximately 1.95 times lighter than lead. This composite reached approximately 69% of the lead's performance with the same thickness in the high energy region where IEMR shielding was the most difficult.

The RWO60 composite showed the highest μ_M value among other composites with its low density that is approximately 2.4 times lower than lead. This value was found to be higher than lead for the low and high IEMR energy region and almost equal to the lead for the medium energy region.

This result shows that if a wearable RWO60 shielding is produced with the same shielding performance with commercial lead aprons, it will be approximately 2 times lighter. Considering that an adult lead apron weighs an average of 10 kg, it is a great advantage that RWO60 aprons increase the user's mobility, bring two times less weight to the body and are comfortable. In addition, since lead

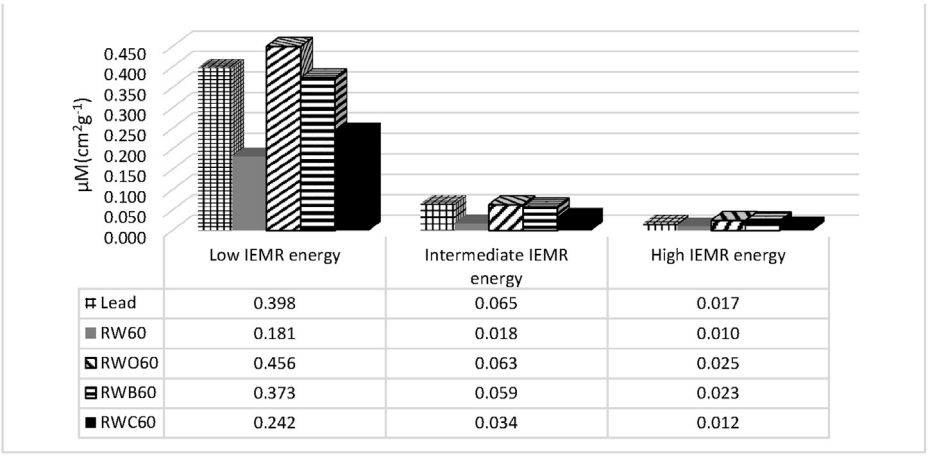

Fig. 9. μ_M (cm^2g^{-1}) values of lead and 60% reinforced composites.

Table 5
Average performance of lead and composites in the low, medium and high IEMR energy regions for unit thickness (F%) and unit mass (cm^2g^{-1}).

Shielding material	Attenuation ratio (%)			Mass attenuation coefficient (cm^2g^{-1})		
	Low IEMR energy	Intermediate IEMR energy	High IEMR energy	Low IEMR energy	Intermediate IEMR energy	High IEMR energy
RW60	85.32	33.57	23.92	0.181	0.018	0.010
RWO60	85.61	41.68	25.10	0.456	0.063	0.025
RWB60	84.87	44.58	26.01	0.373	0.059	0.023
RWC60	90.92	42.99	22.90	0.242	0.034	0.012
Pb	99.98	67.68	37.71	0.398	0.065	0.017

is a material that can be easily deformed by mechanical effects, it must be renewed frequently to avoid performance deterioration while the proposed polymer matrix composite material has high stability. Another important advantage of the proposed material is human health and environmental friendliness. Due to its high toxicity, lead harms both human health and the environment during its usage and production. Although tungsten is an expensive material, the lightness, strength and non-toxic properties of the proposed composite make it superior to lead.

Declaration of competing interest

The authors declare that they have no known competing financial interests or personal relationships that could have appeared to influence the work reported in this paper.

Acknowledgements

The authors would like to acknowledge the financial assistance of the Mugla Sitki Kocman University through the Grant 2014/016.

References

[1] TAEK, Ögrenci Kösesi, Bölüm 3- Radyasyon "Radyasyon ve Biz". http://www.taek.gov.tr/ogrenci/r08.htm. (Accessed 10 January 2020).
[2] Jun-Hua Liu, Quan-Ping Zhang, Nan Sun, Yang Zhao, Rui Shi, Yuan-Lin Zhou, Jian Zheng, Elevated gamma-rays shielding property in lead-free bismuth tungstate by nanofabricating structures, J. Phys. Chem. Solid. 112 (2018) 185–189.
[3] Quan-Ping Zhang, Yun-Chuan Xu, Jia-Le Li, Ao-Jie Liu, Dui-Gong Xu, Wei Ming, Yuan-Lin Zhou, Hunting for advanced low-energy gamma-rays shielding materials based on PbWO4 through crystal defect engineering, J. Alloys Compd. 822 (2020) 153737.
[4] Yun-Chuan Xu, Chi Song, Xiao-Yong Ding, Yang Zhao, Dui-Gong Xu, Quan-Ping Zhang, Yuan-Lin Zhou, Tailoring lattices of Bi2WO6 crystals via Ce doping to improve the shielding properties against low-energy gamma rays, J. Phys. Chem. Solid. 127 (2019) 76–80.
[5] MTA, Maden Tetkik ve Arama Genel Müdürlüğü, 2020. https://www.mta.gov.tr/v3.0/bilgi-merkezi/tungsten-volfram. (Accessed 8 January 2020).
[6] Center of China Tungsten Industry Association, Tungsten alloy material. http://www.tungstencopper.net/Tungsten-alloymaterial/default.htm. (Accessed 4 March 2016).
[7] S. Kobayashi, N. Hosoda, R. Takashima, Tungsten alloys as radiation protection materials, Nucl. Instrum. Methods Phys. Res. 390 (1997) 426–430.
[8] L.W. Lee, Shielding Analysis of a Small Compact Space Nuclear Reactor, Air Force Weapons Laboratory, Kirtland Air Force Base, NM, AFWL-TR-87-94, 1987.
[9] G. Friedlander, J.W. Kennedy, E.S. Macias, J.M. Miller, Nuclear and Radiochemistry, Wiley, New York, 1981.
[10] Poliya, Poliester ürün teknik bülteni, doc.cod UTB Polives Ver 2012-Polipol Rv, Ver, 2012.
[11] E. Eren Belgin, G.A. Ayçık, Preparation and radiation attenuation performances of metal oxide filled polyethylene based composites for ionizing electromagnetic radiation shielding applications, J. Radioanal. Nucl. Chem. 306 (2015) 107–117.
[12] E. Eren Belgin, G.A. Aycik, A. Kalemtas, A. Pelit, D.A. Dilek, M.T. Kavak, Preparation and characterization of a novel ionizing electromagnetic radiation shielding material; hematite filled polyester based composites, Radiat. Phys. Chem. 115 (2015) 43–48.
[13] E. Eren Belgin, G.A. Aycik, A. Kalemtas, A. Pelit, D.A. Dilek, M.T. Kavak, Usability of natural titanium-iron oxide as filler material for ionizing electromagnetic radiation shielding composites; preparation, characterization and performance, J. Radioanal. Nucl. Chem. 309 (2016) 659–666.
[14] K. Kirdsiri, J. Kaewkhao, A. Pokaipisit, W. Chewpraditkul, P. Limsuwan, Gamma-rays shielding properties of xPbO:(100−x)B2O3 glasses system at 662 keV, Ann. Nucl. Energy 36 (2009) 1360–1365.